Pair-hypernetted-chain closure for three-body potentials: Results for argon with the Axilrod-Teller triple-dipole potential

Phil Attard*

Department of Chemistry, University of British Columbia, Vancouver, British Columbia, Canada V6T 1Y6
(Received 8 July 1991)

The hypernetted-chain closure is modified to include three-body potentials. The latter is reduced to a state-dependent effective pair potential. Explicit expressions for the Helmholtz free energy and for the chemical potential are derived for the modified closure. The approximation is shown to be relatively self-consistent and in qualitative agreement with perturbation results. An argonlike fluid is discussed using the Lennard-Jones pair potential and the Axilrod-Teller triple-dipole potential. In agreement with earlier work, it is found that the effective three-body contribution is positive, increasing the pressure and the internal energy by about 10% in the liquid state.

I. INTRODUCTION

According to statistical mechanics, the macroscopic properties of matter can be calculated from the microscopic interaction potentials between molecules. Two obstacles hinder the realization of this goal: the intermolecular potential may be difficult to measure or calculate, and the usual approximation schemes of statistical mechanics may be inappropriate or intractable for realistic potentials. The latter is currently the proximate impediment to a satisfactory description of simple fluids.

An example of the progress that has been made is provided by argon, for which the intermolecular potential is reasonably well characterized [1]. At long range the functional form and the magnitude of the potential can be calculated exactly. This is the dispersion energy, which arises from correlated fluctuations of the electron clouds of the atoms, and, in addition to the well-known r^{-6} pair term, it includes the Axilrod-Teller triple-dipole three-body contribution [2]. The short-range repulsion, often modeled by an r^{-12} term, is essentially the Pauli exclusion of the overlapping electron clouds, and can only be approximately calculated. Here, too, three-body effects have been described [3]. Although the small separation regime is problematic for theoretical calculations, the potential here and in the region of its minimum may be experimentally measured [1].

Nowadays, it must be regarded as routine to calculate the macroscopic properties of classical, equilibrium, bulk, simple fluids that interact with given pairwise additive potentials. However, three-body contributions pose great challenges, not so much to the formalism of statistical mechanics, but to its practical application. With one exception [4], no simulation or integral-equation results for real fluids have so far been reported. It is now some time since Barker and co-workers [5,6] performed a perturbation calculation with reference to pairwise additive argon and concluded that the effects of the Axilrod-Teller triple-dipole potential were non-negligible. It seems timely to explore practical theoretical approaches for simple fluids that interact with three-body potentials, since this is necessary before the goal discussed in the first paragraph can be achieved.

The approach to three-body potentials taken in this paper is based upon the well-known hypernetted-chain (HNC) closure to the Ornstein-Zernike integral equation. Like the HNC, the new closure neglects the bridge function (thereby yielding only the third virial coefficient exactly), while retaining some contributions from all orders in density, which hopefully assures its reliability at liquid-like densities. The three-body potential enters as a state-dependent pair potential that is determined as part of the iterative solution of the Ornstein-Zernike equation. This reduction of the three-body potential, and also the determination of the virial pressure and of the internal energy, involves a three-dimensional quadrature, but the scheme still remains hardly more complex than a normal pair-HNC computation. The great advantage of the method, which may be regarded as the simplest nontrivial approximation for fluids with three-body potentials, is that it is so tractable; even the curve fitting of relatively complicated effective two- and three-body potentials to experimental data should be feasible.

The second part of this paper contains specific results for an argonlike fluid. The calculations are intended to illustrate the changes caused by the inclusion of the asymptotic three-body potential. To this end the Lennard-Jones pair potential has been used, with the magnitude of the long-range part equaling the proper argon pair-dispersion potential. The three-body potential employed is the triple-dipole potential of Axilrod and Teller [2], with the magnitude again coming from a first-principles calculation. The conclusions drawn here are consonant with those of Barker and co-workers [5,6], namely, that the three-body potential can contribute several percent to the bulk properties of the fluid.

II. THEORY

A. Closure approximation

Modern theories of the liquid state that are based upon particle distribution functions start from the Ornstein-

Zernike equation. This relates the total, $h(r)$, and the direct, $c(r)$, pair-correlation functions [7]

$$h(r_{12}) = c(r_{12}) + \rho \int h(r_{13})c(r_{32})d\mathbf{r}_3 \ , \tag{1}$$

where ρ is the number density. This paper focus on uniform one-component fluids composed of spherical atoms; the generalization to other situations appears straightforward. The Ornstein-Zernike equation has the effect of connecting Yvon-Mayer cluster diagrams in series at nodal points.

The hypernetted-chain closure approximates the pair potential of mean force, $w(r_{12})$. This connects diagrams in parallel, since it is the exponential of $w(r_{12})$ that yields the radial distribution function $g_2(r_{12}) = h(r_{12}) + 1$. For the case of a fluid interacting only with two-body potentials, the pair potential of mean force consists of the pair potential $u_2(r_{12})$, the Ornstein-Zernike series function $h(r_{12}) - c(r_{12})$, and the bridge function. If in addition to the two-body potential there is a three-body potential, extra diagrams contribute to the potential of mean force, including implicit contributions to the series function and to the bridge function, and explicit series diagrams not of the Ornstein-Zernike type. The approximation to be made is to neglect all bridge diagrams, and to retain only those of the latter series diagrams that involve an integral over a single root point at a time. The neglected diagrams are at least of order ρ^2. The series diagrams that are retained, in addition to the Ornstein-Zernike ones, may be exactly resummed and are represented by two root points and a single field point, all directly connected by the three-body Mayer-f function and by two radial distribution functions. The result is

$$\beta \bar{u}(r_{12}) \equiv -\rho \int \{ -1 + \exp[-\beta u_3(\mathbf{r}_{31}, \mathbf{r}_{32})] \}$$

$$\times g_2(r_{31})g_2(r_{32})d\mathbf{r}_3 \ , \tag{2}$$

where $\beta = 1/k_B T$, k_B being Boltzmann's constant and T the absolute temperature. For the fluids considered here, the three-body potential $u_3(\mathbf{r}_1, \mathbf{r}_2, \mathbf{r}_3)$ depends only upon the triangle (e.g., any two sides and the included angle) formed by the three atoms.

The new closure approximation for three-body potentials is

$$\beta w(r_{12}) = \beta u_2(r_{12}) + \beta \bar{u}(r_{12}) - [h(r_{12}) - c(r_{12})] \ , \tag{3}$$

where the bridge function and certain non-Ornstein-Zernike-series diagrams have been neglected. This approximation may be stated in other words, namely, that it retains all diagrams, but only those diagrams that can be computed by storing only two-body functions and by doing single-particle integrals. The total-correlation function is given by

$$h(r_{12}) = -1 + \exp[-\beta w(r_{12})] \ . \tag{4}$$

These four equations, which relate four unknown functions, are readily solved by iteration using the techniques standardized from the usual HNC closure [the quadrature in Eq. (2) is discussed below]. The three-body potential has been reduced to a state-dependent effective pair potential. The neglected functions are of second order in

density, and so the radial distribution function is given exactly to linear order in density by this approximation; this would not be the case if the three-body potential were simply neglected. In the absence of three-body potentials, the closure reduces to the standard HNC for fluids interacting with pair potentials.

The HNC approximation for fluids with pairwise additive potentials deteriorates at higher densities, and there have been a number of improvements, including the explicit calculation of the bridge function [8–11]. Of particular interest in the present context is the reference hypernetted-chain (RHNC) method, where the (known) bridge function of some simpler fluid (e.g., hard sphere) is used [12,13]. Since the RHNC treats the underlying pair fluid more accurately, it could be a worthwhile modification of the scheme given above for fluids with three-body potentials, particularly since it would not increase the computational complexity of the approach.

Silvera and Goldman [14] (see also Ref. [15]) have also reduced the three-body potential to an effective pair potential, but their expression is different from Eq. (2). For the Axilrod-Teller triple-dipole potential, they choose a plausible but *ad hoc* $C_9 r^{-9}$ pair potential, with the density-independent coefficient fixed to give the correct cohesive energy of the crystal at a single state point. Because the near-neighbor distance scales with the inverse cube root of the density, their effective pair potential will give a contribution to the lattice energy which goes as the third power of density, which is correct. Similarly, the effective pair potential derived here, Eq. (2), which is linear in density to leading order at low densities, gives a contribution to the internal energy of dilute gases that is cubic in density, which is also correct. One cannot say how it would contribute to the cohesive energy of the solid because of the unknown density dependence of the particle distribution functions which occur in Eq. (2), and also because the closure approximation, Eq. (3), is not expected to be valid at solid densities. Below it is argued that the effective pair potential, Eq. (2), decays like r^{-6} at large separations, which is probably exact for a dilute gas. That this disagrees with the r^{-9} form of Silvera and Goldman [14] may not be significant because they apply their approximation to solids where the near-neighbor contribution dominates the cohesive energy. If their potential were changed to an $A_6 r^{-6}$ potential, with the coefficient A_6 being linear in density, one would still obtain a lattice energy that depended upon the third power of density.

B. Thermodynamic quantities

It will prove convenient to specify the various three-particle functions in terms of the triangle formed by the molecules, $f_3(\mathbf{r}_1, \mathbf{r}_2, \mathbf{r}_3) = f_3(s, t, x)$. Here $t = |\mathbf{r}_1 - \mathbf{r}_2|/2$ is half the length of one of the sides, $s = |\mathbf{r}_3 - (\mathbf{r}_1 + \mathbf{r}_2)/2|$ is the distance from the midpoint of this side to the remaining vertex, and $x = \mathbf{s} \cdot \mathbf{t}/st$ is the cosine of the angle between these two vectors. From symmetry, $f_3(s, t, x) = f_3(s, t, -x)$.

The excess internal energy per atom is easily shown to be

$$U^{ex}/N = \frac{\rho}{2!}\int d\mathbf{r}_{12}g_2(r_{12})u_2(r_{12}) + \frac{\rho^2}{3!}\int d\mathbf{r}_{12}d\mathbf{r}_{13}g_3(\mathbf{r}_{12},\mathbf{r}_{13})u_3(\mathbf{r}_{12},\mathbf{r}_{13})$$

$$= 2\pi\rho\int_0^\infty g_2(r)u_2(r)r^2 dr + \frac{2^6\pi^2\rho^2}{3}\int_0^\infty ds\, s^2\int_0^\infty dt\, t^2\int_0^1 dx\, g_3(s,t,x)u_3(s,t,x) , \tag{5}$$

and the virial pressure is

$$P_v = \rho k_B T - \frac{\rho^2}{2!3}\int d\mathbf{r}_{12}g_2(\mathbf{r}_{12})\mathbf{r}_{12}\cdot\nabla_{\mathbf{r}_{12}}u_2(r_{12}) - \frac{\rho^3}{3!3}\int d\mathbf{r}_{12}d\mathbf{r}_{13}g_3(\mathbf{r}_{12},\mathbf{r}_{13})\mathbf{r}_{12}\cdot\nabla_{\mathbf{r}_{12}}u_3(\mathbf{r}_{12},\mathbf{r}_{13})$$

$$= \rho k_B T - \frac{2\pi\rho^2}{3}\int_0^\infty g_2(r)r\frac{\partial u_2(r)}{\partial r}r^2 dr - \frac{2^6\pi^2\rho^3}{9}\int_0^\infty ds\, s^2\int_0^\infty dt\, t^2\int_0^1 dx\, g_3(s,t,x)t\frac{\partial u_3(s,t,x)}{\partial t} . \tag{6}$$

Here $g_3(\mathbf{r}_1,\mathbf{r}_2,\mathbf{r}_3)$ is the three-particle distribution function, which will be approximated below.

The excess chemical potential can be written in terms of a coupling constant integral,

$$B\mu^{ex} = \rho\int_0^1 d\lambda\int d\mathbf{r}_{12}g_2^{(\lambda)}(r_{12})\beta u_2(r_{12})$$

$$+ \frac{\rho^2}{2!}\int_0^1 d\lambda\int d\mathbf{r}_{12}d\mathbf{r}_{13}g_3^{(\lambda)}(\mathbf{r}_{12},\mathbf{r}_{13})\beta u_3(\mathbf{r}_{12},\mathbf{r}_{13}) . \tag{7}$$

Here only the particle at $\mathbf{r}_1$ is partially coupled; at $\lambda=0$ it is absent, and at $\lambda=1$ it is an ordinary atom of the fluid. On the other hand, the coupling constant for the excess Helmholtz free energy per atom couples all particles simultaneously,

$$\beta A^{ex}/N = \frac{\rho}{2!}\int_0^1 d\lambda\int d\mathbf{r}_{12}g_2^{(\lambda)}(r_{12})\beta u_2(r_{12})$$

$$+ \frac{\rho^2}{3!}\int_0^1 d\lambda\int d\mathbf{r}_{12}d\mathbf{r}_{13}g_3^{(\lambda)}(\mathbf{r}_{12},\mathbf{r}_{13})$$

$$\times\beta u_3(\mathbf{r}_{12},\mathbf{r}_{13}) . \tag{8}$$

Equations (7) and (8) are straightforward generalizations of the well-known expressions for fluids that interact with only pair potentials.

These four expression, Eqs. (5)–(8), are formally exact. They each explicitly contain two- and three-body terms, which depend on the pair and triplet distribution functions. Note that even if the triplet term were neglected (in many situations the pair term gives the dominant contribution), the three-body potential would still have an effect via the radial distribution function. In practice one must approximate the particle distribution functions. An approximation for the radial distribution function was given above, and it remains to specify the three-particle distribution function.

In this work the Kirkwood superposition approximation [16] will be used,

$$g_3(\mathbf{r}_{12},\mathbf{r}_{13}) = g_2(r_{12})g_2(r_{13})g_2(r_{23})\exp[-\beta u_3(\mathbf{r}_{12},\mathbf{r}_{13})] . \tag{9}$$

There are several reasons for choosing this simplest approximation, not least of which is the goal of a tractable practical theory for fluids with three-body potentials. Moreover, with this approximation the virial pressure remains exact to third order in density. Finally, it turns out that one can actually perform the coupling-constant integrals for the chemical potential and for the free energy when the superposition approximation is used in conjunction with the closure approximation given in Sec. II A. This is a desirable attribute that suggests a certain consistency in the two approximations.

C. Chemical potential

The pair contribution to the chemical potential, Eq. (7), is most easily evaluated by utilizing the differential of the closure relation, Eq. (4),

$$\beta u_2(r_{12})g_2^{(\lambda)}(r_{12}) = \frac{-\partial g_2^{(\lambda)}(r_{12})}{\partial\lambda}$$

$$+ g_2^{(\lambda)}(r_{12})\frac{\partial}{\partial\lambda}[h^{(\lambda)}(r_{12})-c^{(\lambda)}(r_{12})]$$

$$- g_2^{(\lambda)}(r_{12})\frac{\partial\beta\bar{u}^\lambda(r_{12})}{\partial\lambda} . \tag{10}$$

Note that here and in Eq. (7) a linear coupling for the pair potential has been chosen, $u_2^{(\lambda)}(r)=\lambda u_2(r)$, and similarly for the three-body potential. Apart from the effective pair potential term, this is the usual HNC expression for which it is possible to perform the coupling-constant integral [17–19],

$$\beta\mu_{HNC}^{ex} = \rho\int_0^1 d\lambda\int d\mathbf{r}_{12}\left[\frac{-\partial g_2^{(\lambda)}(r_{12})}{\partial\lambda} + g_2^{(\lambda)}(r_{12})\frac{\partial}{\partial\lambda}[h^{(\lambda)}(r_{12})-c^{(\lambda)}(r_{12})]\right]$$

$$= \rho\int d\mathbf{r}_{12}[-c(r_{12})+h(r_{12})^2/2 - h(r_{12})c(r_{12})/2] . \tag{11}$$

The last term, which represents loops of c bonds, was integrated by noting that only the particle at $\mathbf{r}_1$ is partially coupled.

Now one has, from Eq. (2),

$$\frac{\partial \beta \bar{u}^{(\lambda)}(r_{12})}{\partial \lambda} = \rho \int d\mathbf{r}_3 \beta u_3(\mathbf{r}_{31}, \mathbf{r}_{32}) e^{-\beta \lambda u_3(\mathbf{r}_{31}, \mathbf{r}_{32})} g_2^{(\lambda)}(r_{31}) g_2(r_{32}) - \rho \int d\mathbf{r}_3 (e^{-\beta \lambda u_3(\mathbf{r}_{31}, \mathbf{r}_{32})} - 1) \frac{\partial g_2^{(\lambda)}(r_{31})}{\partial \lambda} g_2(r_{32}) \; ,$$

(12)

and also, from Eq. (9),

$$g_3^{(\lambda)}(\mathbf{r}_{31}, \mathbf{r}_{32}) = g_2^{(\lambda)}(r_{12}) g_2^{(\lambda)}(r_{13}) g_2(r_{23}) e^{-\beta u_3(\mathbf{r}_{31}, \mathbf{r}_{32})} \; .$$

(13)

The excess chemical potential, Eq. (7), now reads

$$\beta \mu^{\mathrm{ex}} - \beta \mu_{\mathrm{HNC}}^{\mathrm{ex}} = -\rho^2 \int_0^1 d\lambda \int d\mathbf{r}_{12} d\mathbf{r}_{13} \left[\frac{1}{2} \beta u_3(\mathbf{r}_{31}, \mathbf{r}_{32}) e^{-\beta \lambda u_3(\mathbf{r}_{31}, \mathbf{r}_{32})} g_2^{(\lambda)}(r_{12}) g_2^{(\lambda)}(r_{13}) g_2(r_{32}) \right.$$

$$\left. - (e^{-\beta \lambda u_3(\mathbf{r}_{31}, \mathbf{r}_{32})} - 1) g_2^{(\lambda)}(r_{12}) \frac{\partial g_2^{(\lambda)}(r_{13})}{\partial \lambda} g_2(r_{32}) \right] \; .$$

(14)

Integrating the second term in the parentheses by parts, one can easily show that

$$I \equiv \int_0^1 d\lambda \left[\frac{1}{2} \beta u_3(\mathbf{r}_{31}, \mathbf{r}_{32}) e^{-\beta \lambda u_3(\mathbf{r}_{31}, \mathbf{r}_{32})} g_2^{(\lambda)}(r_{12}) g_2^{(\lambda)}(r_{13}) g_2(r_{32}) \right.$$

$$\left. - (e^{-\beta \lambda u_3(\mathbf{r}_{31}, \mathbf{r}_{32})} - 1) g_2^{(\lambda)}(r_{12}) \frac{\partial g_2^{(\lambda)}(r_{13})}{\partial \lambda} g_2(r_{32}) \right]$$

$$= -(e^{-\beta u_3(\mathbf{r}_{31}, \mathbf{r}_{32})} - 1) g_2(r_{12}) g_2(r_{13}) g_2(r_{32}) - I \; .$$

(15)

It follows that

$$\beta \mu^{\mathrm{ex}} = \beta \mu_{\mathrm{HNC}}^{\mathrm{ex}} + \frac{\rho^2}{2} \int d\mathbf{r}_{12} d\mathbf{r}_{13} (e^{-\beta u_3(\mathbf{r}_{31}, \mathbf{r}_{32})} - 1) g_2(r_{12}) g_2(r_{13}) g_2(r_{32})$$

$$= 2\pi \rho \int_0^\infty [h(r)^2 - h(r) c(r) - 2c(r) - \beta \bar{u}(r) g_2(r)] r^2 dr \; .$$

(16)

D. Free energy

The evaluation of the coupling-constant integral for the excess Helmholtz free energy, Eq. (8), is very similar to that for the chemical potential. One treats the HNC contribution to the pair part using Eq. (10) as before, except that now all the c bonds in the loop term depend upon the coupling constant (because all particles in the fluid are simultaneously coupled). This term may be evaluated in Fourier space using Parsevaal's theorem and the Ornstein-Zernike equation,

$$\frac{\rho}{2} \int_0^1 d\lambda \int d\mathbf{r}_{12} h^{(\lambda)}(r_{12}) \frac{\partial c^{(\lambda)}(r_{12})}{\partial \lambda} = \frac{\rho}{16\pi^3} \int_0^1 d\lambda \int d\mathbf{k} \frac{\hat{c}^{(\lambda)}(k)}{1 - \rho \hat{c}^{(\lambda)}(k)} \frac{\partial \hat{c}^{(\lambda)}(k)}{\partial \lambda}$$

$$= \frac{-1}{16\pi^3} \int d\mathbf{k} \{ \hat{c}(k) + \rho^{-1} \ln[1 - \rho \hat{c}(k)] \} \; .$$

(17)

Hence the HNC contribution is [17,18]

$$\beta A_{\mathrm{HNC}}^{\mathrm{ex}} / N = \frac{\rho}{2} \int d\mathbf{r}_{12} [h(r_{12})^2 / 2 - c(r_{12})] + \frac{1}{16\pi^3} \int d\mathbf{k} \{ \hat{c}(k) + \rho^{-1} \ln[1 - \rho \hat{c}(k)] \} \; .$$

(18)

One now has

$$\frac{\partial \beta \bar{u}^{(\lambda)}(r_{12})}{\partial \lambda} = \rho \int d\mathbf{r}_3 \beta u_3(\mathbf{r}_{31}, \mathbf{r}_{32}) e^{-\beta \lambda u_3(\mathbf{r}_{31}, \mathbf{r}_{32})} g_2^{(\lambda)}(r_{31}) g_2^{(\lambda)}(r_{32}) - 2\rho \int d\mathbf{r}_3 (e^{-\beta \lambda u_3(\mathbf{r}_{31}, \mathbf{r}_{32})} - 1) \frac{\partial g_2^{(\lambda)}(r_{31})}{\partial \lambda} g_2^{(\lambda)}(r_{32}) \; ,$$

(19)

and also,

$$g_3^{(\lambda)}(\mathbf{r}_{31}, \mathbf{r}_{32}) = g_2^{(\lambda)}(r_{12}) g_2^{(\lambda)}(r_{13}) g_2^{(\lambda)}(r_{32}) e^{-\beta u_3(\mathbf{r}_{31}, \mathbf{r}_{32})} \; .$$

(20)

The excess Helmholtz free energy per particle now reads

$$\beta A^{ex}/N - \beta A_{HNC}^{ex}/N = \rho^2 \int_0^1 d\lambda \int d\mathbf{r}_{12}d\mathbf{r}_{13} \left[\frac{-\beta}{3} u_3(\mathbf{r}_{31},\mathbf{r}_{32})e^{-\beta\lambda u_3(\mathbf{r}_{31},\mathbf{r}_{32})} g_2^{(\lambda)}(r_{12})g_2^{(\lambda)}(r_{13})g_2^{(\lambda)}(r_{32}) \right.$$

$$\left. + (e^{-\beta\lambda u_3(\mathbf{r}_{31},\mathbf{r}_{32})}-1)g_2^{(\lambda)}(r_{12})\frac{\partial g_2^{(\lambda)}(r_{13})}{\partial\lambda}g_2^{(\lambda)}(r_{32}) \right] . \qquad (21)$$

Again integrating the second term in the parentheses by parts, one has

$$I \equiv \int_0^1 d\lambda \left[\frac{-\beta}{3} u_3(\mathbf{r}_{31},\mathbf{r}_{32})e^{-\beta\lambda u_3(\mathbf{r}_{31},\mathbf{r}_{32})} g_2^{(\lambda)}(r_{12})g_2^{(\lambda)}(r_{13})g_2^{(\lambda)}(r_{32}) \right.$$

$$\left. + (e^{-\beta\lambda u_3(\mathbf{r}_{31},\mathbf{r}_{32})}-1)g_2^{(\lambda)}(r_{12})\frac{\partial g_2^{(\lambda)}(r_{13})}{\partial\lambda}g_2^{(\lambda)}(r_{32}) \right]$$

$$= (e^{-\beta u_3(\mathbf{r}_{31},\mathbf{r}_{32})}-1)g_2(r_{12})g_2(r_{13})g_2(r_{32})-2I . \qquad (22)$$

The final result for the free energy is

$$\beta A^{ex}/N = \beta A_{HNC}^{ex}/N + \frac{\rho^2}{3} \int d\mathbf{r}_{12}d\mathbf{r}_{13}(e^{-\beta u_3(\mathbf{r}_{31},\mathbf{r}_{32})}-1)g_2(r_{12})g_2(r_{13})g_2(r_{32})$$

$$= 2\pi\rho \int_0^\infty [\tfrac{1}{2}h(r)^2 - c(r) - \tfrac{2}{3}\beta\bar{u}(r)g_2(r)]r^2 dr + \frac{1}{4\pi^2} \int_0^\infty \{\hat{c}(k)+\rho^{-1}\ln[1-\rho\hat{c}(k)]\}k^2 dk . \qquad (23)$$

E. Thermodynamic pathways

One reason that the closed expression for the free energy is convenient is that it provides an alternative route to some of the thermodynamic quantities. This is often a useful guide to the accuracy of an approximation. One example is the compressibility factor, $z \equiv P/\rho k_B T$, which can be obtained from the virial, Eq. (6), or from the density derivative of the free energy

$$z_a = \frac{-1}{\rho k_B T} \left[\frac{\partial A}{\partial V} \right]_{N,T}$$

$$= 1 + \rho \left[\frac{\partial a^{ex}}{\partial\rho} \right]_T , \qquad (24)$$

where $a^{ex}(\rho,T) \equiv \beta A^{ex}/N$.

Similarly the excess chemical potential can be obtained from

$$\beta\mu_a^{ex} = a^{ex} + \rho \left[\frac{\partial a^{ex}}{\partial\rho} \right]_T . \qquad (25)$$

It is worth mentioning that there is some numerical evidence that this pathway, using the approximation (23) for the excess free energy, is precisely equivalent to the approximation (16) for the chemical potential when the closure (3) is used.

Another quantity of interest is the dimensionless isothermal compressibility

$$\kappa_T = k s_B T \left[\frac{\partial\rho}{\partial P} \right]_T , \qquad (26)$$

which diverges along the spinodal line and at the critical point. It may be evaluated from the integral of the total-correlation function

$$\kappa_T^0 = 1 + 4\pi\rho \int_0^\infty h(r)r^2 dr , \qquad (27)$$

or from the density derivative of the pressure

$$\kappa_T^v = \left[z_v + \rho \left[\frac{\partial z_v}{\partial\rho} \right]_T \right]^{-1} . \qquad (28)$$

In order to utilize these alternate pathways one requires the density derivative of the Helmholtz free energy and of the virial pressure. This can be done numerically using difference methods, but it is much better to proceed analytically. It is straightforward to differentiate Eqs. (6) and (23) with respect to density, and one sees that the results depend upon the density derivative of the total- and of the direct-correlation functions, and also of the effective pair potential. A closed set of equations for these may be obtained by differentiating the Ornstein-Zernike equation (1) and the closure equations (2)–(4). These new equations can be solved in conjunction with the solution of the undifferentiated equations with little additional effort. The differentials of the pressure and of the free energy may be evaluated at the same time as the quadratures for the undifferentiated quantities.

III. RESULTS FOR AN ARGONLIKE FLUID

A. Potential and numerics

The theory of the preceding section will now be used to calculate the equation of state and other properties of an argonlike fluid. The pair potential used is the Lennard-Jones potential

$$u_2(r) = \frac{C_{12}}{r^{12}} + \frac{C_6}{r^6} , \qquad (29)$$

with $C_6 = -6.48\times10^{-78}$ J m^6 being the argon induced-dipole dispersion coefficient [1]. The short-range repulsion is determined by $C_{12}=2.44\times10^{-136}$ J m^{12}, which corresponds to the usual Lennard-Jones potential $\sigma = 0.335$ nm. These parameters give a pair potential with a

well depth of $\varepsilon/k_B \equiv -C_6/4\sigma^6 k_B = 83$ K, which is somewhat less than the measured 120–140 K [1].

The Axilrod-Teller triple-dipole potential is [2]

$$u_3(\mathbf{r}_1,\mathbf{r}_2,\mathbf{r}_3) = \nu \frac{r_{12}^2 r_{13}^2 r_{23}^2 + 3(\mathbf{r}_{12}\cdot\mathbf{r}_{13})(\mathbf{r}_{21}\cdot\mathbf{r}_{23})(\mathbf{r}_{31}\cdot\mathbf{r}_{32})}{r_{12}^5 r_{13}^5 r_{23}^5}$$

(30)

with $\nu = 7.32\times10^{-108}$ J m^9 [5,20]. This value corresponds to a dimensionless polarizability of $\alpha \approx -4\nu/3C_6\sigma^3 = 0.04$. This potential is positive for most configurations of the three atoms, except for nearly linear ones. In the geometry of Sec. II one has

$$u_3(s,t,x) = \frac{u}{8t^3} \frac{s^4 + 5t^2 s^2 - 2t^4 - t^2 s^2 x^2 - 3s^4 x^2}{[(t^2+s^2)^2 - 4t^2 s^2 x^2]^{5/2}}.$$

(31)

Also,

$$\frac{\partial u_3(s,t,x)}{\partial t} = \frac{3\nu}{8t^4}[(t^2+s^2)^2 - 4t^2 s^2 x^2]^{-7/2}$$

$$\times(6t^8 - 13t^6 s^2 - 25t^4 s^4 - 7t^2 s^6 + 3s^8 x^2 - 7t^6 s^2 x^2 + 27t^2 s^6 x^2 + 57t^4 s^4 x^2 - 8t^4 s^4 x^4 - 32t^2 s^6 x^4 - s^8).$$

(32)

The fluid that interacts only with the pair potential (29) will be referred to as the Lennard-Jones fluid, and the argonlike fluid that in addition includes the triplet potential (30) will be referred to as the Axilrod-Teller fluid.

The resolution of Eqs. (1)–(4) hardly differed from the usual fast-Fourier-transform method that is standard for the Ornstein-Zernike equation and HNC closure. The number of grid points used was 2^{12}, and the mesh in real space was $\Delta r = 0.01\sigma$, giving a cutoff of 40σ. The two-dimensional integrals for $\bar{u}(r)$, Eq. (2), and the three-dimensional integral for the virial pressure and for the internal energy, were evaluated using Gaussian quadratures with 75 nodes in the angular direction, 250 nodes in each radial direction, and a radial cutoff of 8σ. Increasing these to 100, 300, and 9σ, respectively, had a negligible effect along the $T = 100$ K isotherm. These multidimensional integrals were evaluated simultaneously, once every 20–100 iterations of both the Ornstein-Zernike equation and closure; the effective pair potential is relatively insensitive to small changes in $g_2(r)$. About 5–10 such cycles were sufficient for six-figure convergence of the various thermodynamic properties. The density derivatives required for the alternative thermodynamic pathways were evaluated as described in Sec. II D.

B. Equation of state

The equation of state of the Axilrod-Teller fluid, as given by the approximations (3) and (9), and the virial pressure (6), using the two- and three-body potentials (29) and (30), is shown in Fig. 1. At high temperatures, the nearly linear isotherms are indicative of an ideal gas. At lower temperatures, the isotherms exhibit greater curvature but remain monotonically increasing. There is an isotherm between 107 and 105 K that is flat around about $\rho\sigma^3 \approx 0.2$–0.3, and therefore it may be identified with the critical isotherm [21]. Below the critical temperature, the isotherms are disjoint; the end points of each branch demark regimes in which the equations do not possess a solution. Since the isothermal compressibility is found to diverge near the end points, it is appropriate to identify the locus of end points with the spinodal line, the limit of metastability of the fluid [21].

For subcritical temperatures, the fluid is gaseous on the

low-density branch, and liquid on the high. In general the coexistence line lies outside the spinodal line, and the fluid in the region between the two is metastable. The coexistence line is defined by the equality of the pressures and of the chemical potentials of the two phases. For the isotherm $T = 100$ K, the virial pressure at the end of the gaseous branch was higher than that at the end of the liquid branch, thus enabling the necessary matching. This, together with flattening of the viral-pressure isotherms as the spinodal (predicted from the divergence of the integral of the total-correlation function) is approached, indicates a broad consistency between the two routes. However, it was found that the chemical potential, given by the Eq. (16) or by Eq. (25), at the end of the gaseous branch was less than at the liquid-branch end point. This inability to equate chemical potentials within the computationally accessible region is a manifestation of inconsistency in the approximation scheme. Indeed, it was found that the pressure curve given by the derivative of the free energy, Eq. (24), did not flatten at the spinodal, and this is also an inconsistency, but a consistent one. Both these observations indicate that if the unstable region of the fluid could be predicted from the free-energy route, it would be smaller than the present prediction from the virial route. Finally it is worth mentioning that
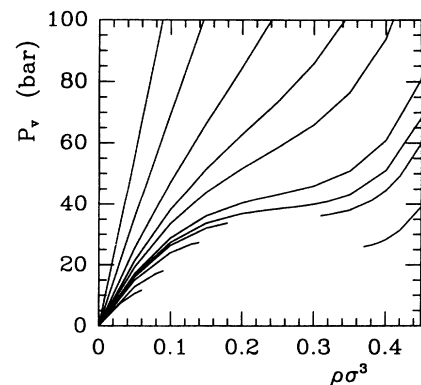

FIG. 1. Theoretical equation of state of the Axilrod-Teller fluid, for isotherms $T = 300$, 200, 150, 130, 120, 110, 107, 105, and 100 K (from top to bottom), and also 90 and 80 K (gaseous only). Note that 1 bar $= 10^5$ N m^{-2} and $\sigma = 0.335$ nm.

the virial pressure was negative for the liquid branch of the isotherms $T = 90$ and 80 K; the pressure from the free energy was positive but larger than that on the gaseous branch.

The equation of state of the Lennard-Jones fluid [parameters as in Eq. (29); no three-body potential] was also calculated (not shown). In this case the closure approximation is just the HNC, and the results are equivalent to those obtained in the pioneering work of Klein and Green [21]. Broadly speaking, the isotherms are similar to those calculated for the argonlike fluid, which includes the Axilrod-Teller triple-dipole potential. The main difference is that the region inaccessible to computation [i.e., the unstable fluid as determined from the divergence of the compressibility, Eq. (27)] is larger for the Lennard-Jones fluid. Also, the subcritical virial isotherms on the liquid branch do not flatten as the spinodal is approached, and the pressure at their end points is substantially higher than that at the end of the gaseous branch. In other words, the approximation for the fluid with three-body interactions shows more consistency between the virial and the compressibility routes on the liquid side of the spinodal than does the HNC approximation for the Lennard-Jones fluid. The reason for this is not understood, and it is probably fortuitous.

The HNC critical temperature of 115–120 K is greater than the exact critical temperature of the Lennard-Jones fluid, $T_c = 105$ K [7]. These may be compared to the theoretical result for the Axilrod-Teller fluid discussed above, $T_c = 150$–107 K, and to the experimental result for argon, $T_c = 150.8$ K. One can see that the critical temperature is quite sensitive to the intermolecular potential, and to the approximation scheme. Indeed, by adjusting the parameters of the Lennard-Jones potential, one can obtain good agreement with experiment, even though the pair potential is incorrect at long range, and three-body effects have not been included. The primary reason that the theoretical result for the Axilrod-Teller fluid ($T_c \approx 106$ K) lies so far below the measured result for argon ($T_c = 150.8$ K) is that the well depth of the Lennard-Jones potential used ($\varepsilon/k_B = 83$ K) is less than the measured 120–140 K. The Lennard-Jones potential is too simple to represent the real pair potential over the whole range [1]. The reason that the Axilrod-Teller fluid has a critical temperature below that of the Lennard-Jones fluid, for the same parameters of the latter potential and for the roughly equivalent HNC-type closure approximation, is that the reduced three-body potential is positive (see below) and competes with the attractive tail of the Lennard-Jones potential.

C. Thermodynamic quantities

The compressibility factor calculated for the Axilrod-Teller fluid and for the Lennard-Jones fluid for the subcritical isotherm $T = 100$ K is shown in Fig. 2. After an initial decrease beneath the ideal-gas value, the pressure increases rapidly in the liquid phase, particularly at the higher densities around σ^{-3}. The self-consistency of the approximate method, Eqs. (3) and (9), as judged from the virial and the free-energy routes, is quite good, the latter
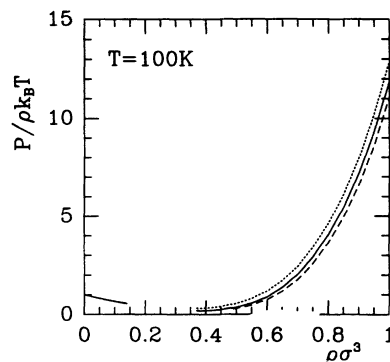

FIG. 2. Compressibility factor given by the virial route [Eq. (6), solid curve], and the free-energy route [Eq. (24), dotted curve]. The dashed curve is the HNC virial result for the Lennard-Jones fluid (no three-body potential).

being about 8% larger at $\rho\sigma^3 = 1.0$. At a higher temperature $T = 120$ K the consistency is about 6% at the same density. The effect of the Axilrod-Teller triple-dipole potential is to increase the pressure compared to the Lennard-Jones fluid. The effect is not large, being about 7% for the virial route and about 15% for the free-energy route at $T = 100$ K. Note that the consistency between these two routes for the HNC description of the Lennard-Jones fluid is such that the two would be indistinguishable on this plot.

The excess internal energy per atom is shown in Fig. 3 for isotherms above and below the critical one. On the liquid branch of the subcritical isotherm, the positive nature of the Axilrod-Teller potential is apparent. Here the internal energy is less negative than for the pure Lennard-Jones fluid. The effect is somewhat larger than for the compressibility factor, being about 15% at $\rho\sigma^3 = 1.0$. On the supercritical isotherm, $T = 120$ K, one draws the same conclusions, while noting that the difference between the two fluids is ameliorated somewhat by the higher temperature. The internal energy reaches a minimum around $\rho\sigma^3 = 0.8$, and then increases as the interactions between the more closely packed atoms are dominated by the positive part of the pair potential.

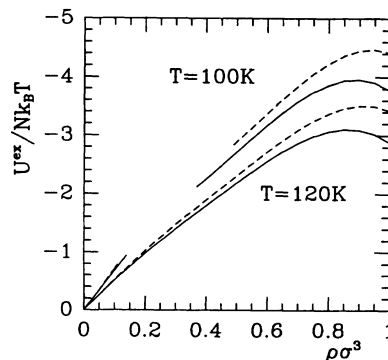Figure 4 exhibits the isothermal compressibility for the

FIG. 3. Excess internal energy per atom for the Axilrod-Teller fluid (solid curves), compared to the fluid interacting only with the Lennard-Jones two-body potential (dashed curves), along two isotherms.
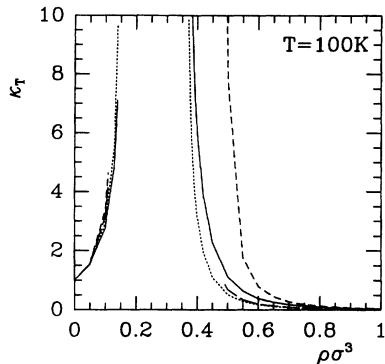
FIG. 4. Dimensionless isothermal compressibility from the integral of the total-correlation function [Eq. (27), solid curve], and from the derivative of the virial pressure [Eq. (28), dotted curve]. The short-dashed and the long-dashed curves are, respectively, the corresponding results for the Lennard-Jones fluid (no three-body potential).

isotherm $T = 100$ K. The divergence as the spinodal is approached is evident, and it allows for a fairly sharp delineation of the stability limit. In the gaseous phase, there is relatively good agreement between the correlation route, Eq. (27), and the virial route, Eq. (28), and also between the Axilrod-Teller fluid and the Lennard-Jones fluid. The liquid branch of the Axilrod-Teller fluid is consistently described by the approximations given here for three-body potentials. On the other hand, the HNC results for the Lennard-Jones liquid provide an illustration of the inconsistency of the two routes that complements the discussion already given in connection with the equation of state. According to the integral of the total-correlation function, the Lennard-Jones fluid is much more compressible than the Axilrod-Teller fluid, and the unstable region of the fluid is much wider. On the supercritical isotherm $T = 120$ K (not shown), the isothermal compressibility peaks at a density around $0.25\sigma^{-3}$, but does not diverge; again the Lennard-Jones fluid described by the correlation route is rather more compressible here than is the Axilrod-Teller fluid.

These results for the thermodynamic quantities may be summarized as follows. The approximation scheme for fluids with three-body potentials appears more self-consistent than the HNC approximation for fluids with pair potentials as far as the isothermal compressibility is concerned (correlation-function route and virial route), but is less self-consistent for the pressure (virial route and free-energy route). The effect of the Axilrod-Teller triple-dipole potential is to increase the pressure, the internal energy, and the resistance to compression, compared to the pure Lennard-Jones fluid. This is not unexpected, since the triple-dipole potential is positive for most configurations of the three atoms, and has been found before [5,22]. On a subcritical isotherm $T = 100$ K, the change can be around 10% at the high density of σ^{-3}, but is no so significant at higher temperatures and at smaller densities.

D. Pair-correlation functions

The radial distribution function is shown in Fig. 5 for gaseous and liquid densities of the subcritical isotherm
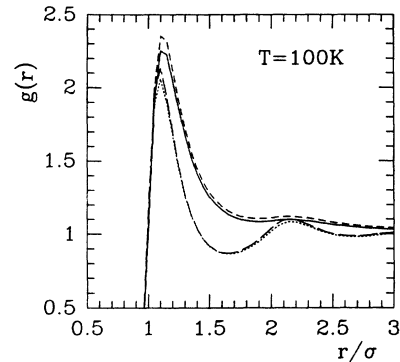

FIG. 5. Radial distribution functions at a subcritical temperature for densities $0.1\sigma^{-3}$ and $0.5\sigma^{-3}$ (pronounced secondary maximum). The solid and dotted curves are for the Axilrod-Teller fluid, and the two dashed curves are for the pure Lennard-Jones fluid.

$T = 100$ K. That $g(r) = 0$, $r \lesssim 0.7\sigma$ indicates a vanishing probability of finding two atoms this close due to the short-range repulsion between them. Beyond the core, one is quite likely to find two atoms in contact, as is manifest by the peak in $g(r)$ at $r \approx 1.1\sigma$. They are drawn in by the attractive tail of the potential and held thereby the thermal pressure of the fluid. The pair distribution function in the gas phase decays more or less monotonically to unity, a value that indicates that the atoms are uncorrelated. The contrasting secondary maximum and other structure, which are characteristic of the liquid phase, are due to solvent packing at the higher density and propagate some distance beyond the originating atom. One expects the pair distribution function to decay to its asymptote at the same rate as the pair potential (r^{-6}), with a magnitude proportional to the isothermal compressibility [11]. As one approaches the spinodal and critical point, $g(r)$ becomes more long ranged, and over substantial separation behaves as an exponential. The decay length diverges near the spinodal, leading to a divergent integral of the total-correlation function for the isothermal compressibility, Eq. (27).

Figure 5 shows that the Axilrod-Teller triple-dipole potential has a fairly small effect on the radial distribution
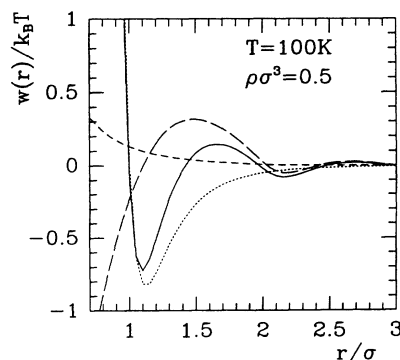

FIG. 6. Contributions to the potential of mean force, Eq. (2). The solid curve is the total $w(r)$, the dotted curve is the Lennard-Jones pair potential $u_2(r)$, the short-dashed curve is the reduced triplet potential $\bar{u}(r)$, and the long-dashed curve is the negative of the series function, $c(r) - h(r)$.
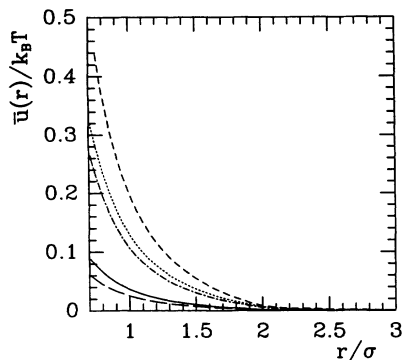
FIG. 7. The reduced three-body potential, Eq. (2). The solid, dotted, and short-dashed curves are for densities of $0.1\sigma^{-3}$, $0.5\sigma^{-3}$, and $0.7\sigma^{-3}$, respectively, at $T = 100$ K. The long-dashed and the dot-dashed curves are for densities of $0.1\sigma^{-3}$ and $0.5\sigma^{-3}$, respectively, at $T = 120$ K.

function. In both the liquid and the gas phase it acts to lower the first peak compared to the Lennard-Jones fluid. The change is greater at the lower density, a result not easy to reconcile with the earlier findings that the three-body potential is more important at higher densities. For the supercritical isotherm $T = 120$ K (not shown), the suppression of the first peak is qualitatively similar but smaller. At this temperature the heights of the contact maxima of the two densities ($0.1\sigma^{-3}$ and $0.5\sigma^{-3}$) coincide, although the higher density still shows an oscillatory structure not evident at the lower density.

Figure 6 shows the various contributions to the pair potential of mean force, Eq. (3). At small separations the steeply repulsive part of the Lennard-Jones potential is dominant, causing the radial distribution function to vanish in the core region. The oscillatory structure in $g(r)$ is due to the series function $h(r) - c(r)$. The reduced three-body potential $\bar{u}(r)$, Eq. (2), is monotonic and positive, giving a repulsive force between two atoms. It is rather small with respect to $k_B T$, but does cause a noticeable decrease in the depth of the well of the potential of mean force compared to that due to the Lennard-Jones pair potential alone. It is this which suppresses the primary maxima in Fig. 5. Thermodynamic quantities such as the internal energy and the virial pressure are rather sensitive to the radial distribution function in this region, a region in which $\bar{u}(r)$, though small, is non-negligible.

The reduced three-body potential $\bar{u}(r)$ is shown in Fig. 7 for various temperatures and densities. The potential is monotonic and positive in all cases. The Axilrod-Teller triple-dipole potential, Eq. (30), is known to be negative for nearly linear configurations of the three atoms (obtuse triangles), but it is positive for the remaining configurations, which are the majority. Hence it is quite reasonable that the integration indicated in Eq. (2) should yield a positive effective pair potential. Further, since there is no direct 12 bond, and because of the averaging implicit in the integration, the monotonic decay is not unexpected even for high densities and subcritical temperatures. Although the Axilrod-Teller three-body potential, Eq. (30), is more short ranged than the Lennard-Jones pair potential, Eq. (29), one anticipates that $\bar{u}(r)$ $\sim r^{-6}$, $r \rightarrow \infty$. This follows from linearization of the ex-

ponential in Eq. (2) and scaling arguments. It is a bit tricky to work out the precise magnitude of this decay. In general the magnitude of $\bar{u}(r)$ increases as the density is increased, and decreases as the temperature is increased. These findings are consistent with the changes in the equation of state and the thermodynamic quantities of the Lennard-Jones fluid observed above.

E. Comparison with a perturbation approximation

Some idea of the accuracy of the approximation scheme given here for fluids that interact with three-body potentials is provided by the self-consistency of the various pathways. One can gain further insight into the reliability of the procedure by comparing with the perturbation results of Barker, Fisher, and Watts [5]. These authors have used the so-called Bobetic-Barker pair potential [23], a 13-parameter potential fitted to the properties of argon. The perturbation approximation consists of an expansion to linear order in v, the coefficient to the Axilrod-Teller triple-dipole potential, Eq. (30). The virial pressure and the internal energy were evaluated as ensemble averages of two- and three-body quantities in the reference fluid, which interacted only with the two-body potential.

In addition to the approximate treatment of the three-body potential, the closure, Eq. (3), also approximates the interactions in the underlying pair fluid. Because this is at the HNC level, it is less reliable at higher densities, quite apart from the approximations in the treatment of the three-body potential. The RHNC method remedies this to some extent by including the bridge function of some reference fluid in the closure, Eq. (3). The most straightforward choice is the hard-sphere bridge function, at the same density as the full fluid, and with a hard-core diameter equal to the zero of the pair potential. Although there exist methods to optimize these parameters [12,13], this simplest prescription was used for the results labeled "RHNC" in Table I, utilizing the HNCP [10] hard-sphere bridge function.

The internal energies given in Table I are in broad agreement, the relative discrepancies being less than 10% for the three approximations. Compared to the pair fluid, the addition of the Axilrod-Teller triple-dipole potential acts to increase the energy, as was concluded earlier in Sec. II C. A large part of the absolute discrepancy for the full fluid is already apparent for the pair fluid. This indicates the error in the HNC at the pair level, an error which is nearly all cases is ameliorated by the RHNC, taking the pair results of Barker, Fisher, and Watts [5] as a benchmark. The change, upon the inclusion of the three-body potential, is predicted by the three approximations to within 10 cal/mol, which suggests that the method of handling three-body potentials by the closure given here is fundamentally reliable for the internal energy.

The pressures predicted by the three approximations in Table I are in much worse agreement than were the internal energies. From the results for the pair fluid, one can reasonably conclude that the HNC is failing at this level, a measure of the sensitivity of the virial pressure to the

TABLE I. Pressure and excess internal energy for an argonlike fluid using the Bobetic-Barker [23] pair potential and the Axilrod-Teller triple-dipole potential (first line of each state point) and for the pair potential only (second line), as given by the linear-perturbation approximation [5], and by the present closures.

T (K)	ρ (cm^3/mol)	Energy (cal/mol)			Pressure (bar)		
		Perturb.	HNC	RHNC	Perturb.	HNC	RHNC
168.86	65.67	-586	-570	-564	90	103	78
			-593	-582		101	74
140.0	41.79	-917	-878	-880	29	145	11
		-954	-914	-911	-34	130	-13
140.0	30.65	-1222	-1123	-1170	618	1163	681
		-1283	-1183	-1229	408	1079	585
100.0	29.66	-1329	-1231	-1268	305	691	270
		-1397	-1295	-1330	58	600	165
100.0	27.04	-1436	-1296	-1362	673	1584	922
		-1523	-1375	-1440	305	1445	769

closure approximation. Although the RHNC certainly improves the agreement with the pair results of Barker, Fisher, and Watts [5], one can have only limited confidence in the closures at high densities on subcritical isotherms. The inclusions of the three-body potential increases the pressure with respect to that of the pair fluid, again in agreement with earlier conclusions. The absolute value of the change can be quite substantial, and may cause concern about the convergence of the perturbation expansion, which retains only the leading term. Nevertheless, the fact that the RHNC lies closer to the perturbation results than the HNC suggests that the pressure in the liquid state is given at least qualitatively correctly by the approximations. Note that the HNC pressures from the virial and the free-energy routes were found to be quite self-consistent for both fluids; obviously one should not take this literally to be the accuracy of the approximation. At the low-density, high-temperature point, there is agreement between all three approximations for the pressure.

A summary of the comparison of the closure with the perturbation approximation is as follows. Both theories are in agreement at high temperatures and low densities. For the liquid state, the internal energies agree, but there are substantial discrepancies for the predictions of the pressure. The major source of disagreement is probably due to the HNC treatment of the underlying pair fluid, which one concludes from the sensitivity of the results to the inclusion of the hard-sphere bridge functions. The changes in the properties of the fluid due specifically to the three-body potential are predicted relatively consistently by the approximations.

It is worth mentioning that the author is currently performing Monte Carlo simulations of the Axilrod-Teller fluid. Preliminary results are in good agreement with the molecular-dynamics simulations of Haile [4], and indicate that the perturbation approximation is very accurate. It appears that the HNC is most reliable at lower densities, and the RHNC improves the closure markedly for the liquid state, as was concluded above.

IV. CONCLUSION

This paper has been concerned with a tractable theory for fluids that interact with three-body potentials, and with the effects of such a potential on an argonlike fluid. The contribution of the three-body potential to the pair potential of mean force was reduced to a state-dependent effective pair potential. This yielded a closure to the Ornstein-Zernike equation similar to the standard hypernetted-chain approximation. An additional approximation—the Kirkwood superposition for the triplet distribution function—was required in order to evaluate the thermodynamic quantities such as the virial pressure and the internal energy. It was found that the superposition approximation complemented the approximate closure in such a way that the coupling-constant integrals could be performed to yield explicit expressions for the chemical potential and for the Helmholtz free energy.

The accuracy of the scheme was partially analyzed by the self-consistency of the different thermodynamic pathways, and by comparison with a perturbation approximation. The closure appears reliable at higher temperatures and in the gas phase. Some caution should be used on the liquid branch of subcritical isotherms, where it appears that there are errors due to the HNC treatment of the underlying pair fluid. The RHNC method offers the possibility of improvement without increasing the computational complexity of the approach. The superposition approximation for the triplet distribution function may also cause errors in the evaluation of thermodynamic quantities. Recent schemes for calculating this function accurately [11,24,25] might conceivably be invoked for this part of the problem. Indeed, the binodal chain method [11] could be modified for three-body potentials, and the calculation of the bridge function and the triplet distribution function would be of comparable complexity to computations already performed for Lennard-Jones fluids [26]. These are fairly demanding, but would provide some greatly desired benchmark results. For the immediate future, the present closure is likely to remain the most tractable approximation for fluids with three-body potentials.

The results for the argonlike fluid illustrated the effects of the three-body potential, rather than providing a quantitative description of experimental data. The simplest two- and three-body potentials (Lennard-Jones and Axilrod-Teller) were used, with parameters fixed by the

asymptotic part of the argon intermolecular potential. The effective pair potential given by the reduction of the Axilrod-Teller triple-dipole potential was found to be positive for all temperatures and densities. Consequently the pressure, the internal energy, and the inverse compressibility were all larger than for the pure Lennard-Jones fluid. The increase was of the order of 10% for the liquid state, but was smaller at higher temperatures and at lower densities. This is in qualitative agreement with the findings of Barker and co-workers [5,6]. The location of the critical point and the spinodal line was found to be quite sensitive to the three-body potential.

In conclusion it is clear that a complete quantitative statistical mechanical description of the macroscopic properties of simple liquids requires at least the two- and three-body contributions to the intermolecular potential. The closure approximation given here represents a step towards that goal.

*Present address: Department of Applied Mathematics, Research School of Physical Sciences, Australian National University, Canberra, Australian Capital Territory 2601, Australia.

[1] G. C. Maitland, M. Rigby, E. B. Smith, and W. A. Wakeham, *Intermolecular Forces* (Clarendon, Oxford, 1981).

[2] B. M. Axilrod and E. Teller, J. Chem, Phys. **11**, 299 (1943).

[3] A. E. Sherwood, A. G. De Rocco, and E. A. Mason, J. Chem. Phys. **44**, 2984 (1966).

[4] J. M. Haile, in *Computer Modelling of Matter*, edited by P. Lykos, ACS Symposium Series Vol. 86 (American Chemical Society, Washington, DC, 1978), p. 172.

[5] J. A. Barker, R. A. Fisher, and R. O. Watts, Mol. Phys. **21**, 657 (1971).

[6] J. A. Barker and M. L. Klein, Phys. Rev. B **7**, 4707 (1973).

[7] J. P. Hansen and I. R. McDonald, *Theory of Simple Liquids* (Academic, New York, 1976).

[8] L. Verlet, Physica **30**, 95 (1964); **31**, 959 (1965).

[9] H. Iyetomi and S. Ichimaru, Phys. Rev. A **27**, 3241 (1983).

[10] P. Attard and G. N. Patey, J. Chem. Phys. **92**, 4970 (1990).

[11] P. Attard, J. Chem. Phys. **93**, 7301 (1990).

[12] F. Lado, Phys. Rev. A **8**, 2548 (1973).

[13] Y. Rosenfeld and N. W. Ashcroft, Phys. Rev. A **20**, 1208 (1979).

[14] I. F. Silvera and V. V. Goldman, J. Chem. Phys. **69**, 4209 (1978).

[15] J. H. Kim, T. Ree, and F. H. Ree, J. Chem. Phys. **91**, 3133 (1989).

[16] J. G. Kirkwood, J. Chem. Phys. **3**, 300 (1935).

[17] T. Morita, Prog. Theor. Phys. **23**, 839 (1960).

[18] O. E. Kiselyov and G. A. Martynov, J. Chem. Phys. **93**, 1942 (1990).

[19] P. Attard, J. Chem. Phys. **94**, 2370 (1991).

[20] R. J. Bell and A. E. Kingston, Proc. Phys. Soc. London **88**, 901 (1966).

[21] M. Klein and M. S. Green, J. Chem. Phys. **39**, 1367 (1963).

[22] J. A. Barker, Phys. Rev. Lett. **57**, 230 (1986).

[23] M. V. Bobetic and J. A. Barker, Phys. Rev. B **2**, 4169 (1970).

[24] P. Attard, J. Chem. Phys. **91**, 3072 (1989).

[25] P. Attard, Mol. Phys. **74**, 547 (1991).

[26] P. Attard, J. Chem. Phys. **89**, 4471 (1991).